Center for Combustion Research

FUNDAMENTAL STUDIES OF ROCKET COMBUSTION CHEMISTRY AND COMBUSTION INSTABILITY

Melvyn C. Branch
John W. Daily
Shankar Mahalingam
Gregory J. Fiechtner

Mechanical Engineering Department
University of Colorado
Boulder, CO 80309-0427

Final Technical Report for 1992
AFOSR Grant No. 90-0121

CCR Report No. 93-01

Center for Combustion Research
University of Colorado
Boulder, CO 80309-0427

University of Colorado at Boulder

REPORT DOCUMENTATION PAGE

Form Approved
OMB No. 0704-0188

1. AGENCY USE ONLY (Leave blank)	2. REPORT DATE	3. REPORT TYPE AND DATES COVERED
	February 1993	Final Technical, 1989-1992

4. TITLE AND SUBTITLE
Fundamental Studies of Rocket Combustion Chemistry and Instability

5. FUNDING NUMBERS
AFOSR 90-0121

6. AUTHOR(S)
M.C. Branch, J.W. Daily, S. Mahalingam, G. Fiechtner

7. PERFORMING ORGANIZATION NAME(S) AND ADDRESS(ES)
Center for Combustion Research
Mechanical Engineering Department
University of Colorado
Boulder, Colorado 80309-0427

8. PERFORMING ORGANIZATION REPORT NUMBER

9. SPONSORING / MONITORING AGENCY NAME(S) AND ADDRESS(ES)
Air Force Office of Scientific Research
Directorate of Aerospace Sciences
Bolling Air Force Base
D.C. 20332-6448

10. SPONSORING / MONITORING AGENCY REPORT NUMBER

11. SUPPLEMENTARY NOTES

12a. DISTRIBUTION / AVAILABILITY STATEMENT
Unclassified; Distribution unlimited.

12b. DISTRIBUTION CODE

13. ABSTRACT *(Maximum 200 words)*

This report provides a summary of results obtained over the past year in fundamental studies of the chemistry of solid rocket combustion and of combustion instability in liquid rocket combustion. A coordinated research program has been initiated to study separate aspects of the complex multidimensional, multiphase and multicomponent reacting flow characteristic of rocket combustion. The focus of the combustion chemistry studies is on flame reactions of gas phase species formed as decomposition products near the surface of the propellant. These flames typically involve a variety of fuel species and nitrogen oxides as oxidizers. The focus of the combustion instability studies is the effect of atomization and vaporization processes on the oscillatory conditions characteristic of combustion instability. The research objectives, progress and research in progress in each of these areas are summarized in the report.

14. SUBJECT TERMS
Rocket Combustion, Combustion Chemistry, Combustion Instability, Droplet Vaporization

15. NUMBER OF PAGES

16. PRICE CODE

17. SECURITY CLASSIFICATION OF REPORT	18. SECURITY CLASSIFICATION OF THIS PAGE	19. SECURITY CLASSIFICATION OF ABSTRACT	20. LIMITATION OF ABSTRACT
Unclassified	Unclassified	Unclassified	

TABLE OF CONTENTS

A. FUNDAMENTAL STUDIES OF ROCKET COMBUSTION CHEMISTRY

A.1 RESEARCH OBJECTIVES

The combustion of solid rocket propellants and other energetic materials is a complex multidimensional and multiphase process involving a wide variety of chemical species. The very high pressure and temperature conditions of practical rocket combustion chambers are at present inaccessible by most conventional diagnostic techniques. The study of these coupled phenomena in situ, therefore, has not been possible in sufficient detail to develop a complete understanding of the chemistry and physics of the combustion process. The objective of most recent studies of the combustion of these materials has been to study separate aspects of the overall process in an effort to provide a comprehensive understanding of the combustion mechanism. This study is one component of that coordinated investigation and has as its focus the gas phase reactions associated with the combustion of these solid fuels.

The decomposition of many of these solid energetic materials during combustion leads to the formation of gaseous hydrocarbon fuel species and oxides of nitrogen which serve as oxidizers (ref. 1 and 2). The reactions of these decomposition products above the propellant surface lead to a gaseous flame which can provide heat which is transferred back to the propellant surface and can thereby influence the burning rate. The purpose of this paper is to summarize the current status of studies we have undertaken of model gas phase flames associated with the combustion of nitramine bases solid rocket propellants. These studies consist of measurements of the structure of stable and unstable species concentration profiles and temperature in laminar, premixed, flat flames of fuel/NO_x mixtures at low pressure. The experimental measurements are then compared to calculations of the concentration profiles using a one dimensional flame code which models the transport processes and chemistry of the flame. The transport processes include species diffusion and thermal conduction through the flame and the chemistry is modeled by a detailed chemical kinetic reaction mechanism.

The basic mechanism used for the modeling work is a subset of the 331-reaction mechanism of Volponi and Branch (ref. 3). Reactions removed were those involving species with low concentrations, including condensed phase molecules, and molecules containing more than three carbon atoms. The resulting mechanism contains 272 reactions. This mechanism was the basis for all of the modeling described in this paper. The flame code used to solve the one dimensional flame equations was by Kee et al. (ref. 4)

A.2 RESEARCH APPROACH AND RECENT RESULTS

A.2.1 FLAMES SUPPORTED BY N_2O AS OXIDIZER

Several recent studies have focused on measuring the temperatures and species concentrations in flames supported by N_2O. Habeebullah et al. (ref. 5), Zabarnick (ref.6), and Vandooren et al. (ref. 7) studied CH_4 reacting with N_2O. Habeebullah measured stable species concentrations using probe sampling, radical species concentrations using laser-induced fluorescence (LIF), and flame temperatures using thermocouples and LIF. Zabarnick used LIF to measure stable and radical species concentrations and flame temperatures. Dindi et al. (ref. 8) studied CO reacting at N_2O, and used probe sampling to measure stable species concentrations, LIF to measure unstable species concentrations, and thermocouples to measure flame temperatures.

We have modeled the structure of all of these flames using our 272 step reaction mechanism. It was

found that in order to have best agreement with the full range of data represented by these results, the rates of several of the reactions needed to be adjusted as indicated in Table 1. The most significant of these changes was for the N_2O decomposition which was adjusted to within the upper range of the literature data for this reaction. This change was needed to model the methane flame data correctly. The other reactions listed in Table I were adjusted to provide good agreement for the CO/N_2O flame data. The results of the modeling for the most important cases studied are given below for the flames with N_2O as oxidizer.

CO-N_2O Flame Structure

Low pressure, laminar, premixed flames of CO-N_2O have been stabilized over a rectangular flat-flame burner (ref. 8). Laser-induced fluorescence spectroscopy was used to establish the absence of CN, CH, NH, NH_2 and OH in these flames. Gas chromatographic sample analysis was used to determine the CO, CO_2, N_2O, NO, N_2 and O_2 concentration profiles for three CO-N_2O flames having equivalent ratios of 1.00, 1.32, 1.50. Lean flames could not be stabilized. Temperature profiles for all three flames were measured using R type thermocouples. Measured temperature profiles were corrected for radiation losses. These flames are considerably lifted above the burner and contain a single luminous zone. The main feature of these flames is the absence of any reactive intermediates except oxygen atom. We have eliminated reactions involving the element H and reduced the 272 step mechanism to 27 reactions. This mechanism was then used to model these CO-N_2O flame data.

A combined "elementary reaction contribution" and "sensitivity" analysis showed that only four of the 27 elementary reactions used in the original kinetic mechanism were important in the production or the consumption of major species in the flame. A comparison of the calculated concentration profiles using the original 27-reaction and the four-reaction mechanisms for all three CO-N_2O flames studied in this investigation showed that the difference between the two profiles was always less than 1% of the total concentration. Hence we propose the following four-step mechanism for the CO-N_2O flames:

$$CO + N_2O \rightarrow CO_2 + N_2$$
$$N_2O + M \rightarrow N_2 + O + M$$
$$N_2O + O \rightarrow N_2 + O_2$$
$$N_2O + O \rightarrow NO + NO$$

The first of the four reactions listed above is the most important reaction for CO-N_2O flames. It accounts for almost all the CO consumption and nearly 90% of the N_2O consumption. The second reaction ($N_2O+M \rightarrow N_2+O+M$) is an important reaction for kineticists. It plays a key role in various environments for NO_x formation or decomposition. It is also used for generating O atoms in studies of elementary oxidation reactions. The last two reactions of the four-step mechanism listed above control the concentration profiles of O_2 and NO.

CH_4-N_2O Flame Structure

Laminar, premixed flat flames of CH_4 with N_2O have been stabilized and studied at 50 torr (ref. 5). This study represents the first nearly complete study of the structure and kinetics of CH_4-N_2O flames including stable and unstable species measurements and detailed chemical kinetic modeling. Three flames were investigated, with slightly fuel rich, near stoichiometric and lean mixtures. Flame modeling has been done using the 272 step reaction mechanism and the reaction mechanism evaluated.

The results of the flame calculations and the experiments are given in Figure 1. The comparison shows good quantitative and qualitative agreement between the measured and calculated profiles especially for stable species. The modeling simulation clearly predicts the general flame structure and species concentration profiles. For the flame radicals, the theoretical results are in good agreement with the experimental results for NH, CN and OH. The computed maximum for the CH radical is shifted in the flame. The exact prediction of the radical concentrations using flame modeling is difficult owing to the high reactivity of these radicals, especially CH.

The reaction mechanism starts with the thermal decomposition of N_2O to N_2 and O which is the initial reaction for radical formation in the flame. The oxygen atom formed from this reaction reacts with H_2 to form a pool of H and OH radicals which then propagate the rest of the mechanism. The results of the sensitivity analysis also shows that N_2O is not totally decomposed to N_2, but it forms some NH and NO molecules directly through reaction with H atoms. The mechanism also shows that methane has a long induction period before being consumed mainly through radical reactions (especially with OH and H) to form methyl (CH_3) intermediate. Once methyl intermediate is formed it has two reaction paths to follow. The first path is to form formaldehyde (CH_2O) which then starts a reaction path to form CO_2. The major reaction for CO conversion to CO_2 in this path is through its reaction with OH radical. The second path that CH_3 follows is to form CH_2^- intermediate which then forms CH through radical reactions. The CH formed through this path reacts with NO from N_2O decomposition to produce NH or CN radicals. This reaction forms the first link in hydrocarbon-nitrogen interactions. The high CN and NH concentration in the flame is attributed to this reaction. However, the reaction of nitrous oxide (N_2O) with H atoms is another important source for the formation of these two radicals (CN and NH). The final products in the exhaust gas were mainly N_2, H_2O, CO and CO_2 with small amounts of NO.

A.2.2 FLAMES SUPPORTED BY NO_2 AS OXIDIZER

Five flames supported by NO_2 as the oxidizer have been studied recently and were tested against our 272 step reaction mechanism. Volponi and Branch (ref. 3 and 9) studied H_2 and C_2H_2 reacting with NO_2 in an argon diluent. They measured stable species concentrations using probe sampling, radical species concentrations using LIF, and flame temperatures using thermocouples and LIF. Branch et al. (ref. 10) studied two different flames supported by NO_2, $CH_4/NO_2/O_2$ and $CH_2O/NO_2/O_2$. They measured stable species concentrations using probe sampling, unstable species concentrations using LIF, and flame temperatures with a thermocouple. Zabarnick (ref. 11) also studied the $CH_4/NO_2/O_2$ flame, using LIF to measure flame temperatures and stable and radical species concentrations. The results of our current modeling of the hydrogen and the acetylene flames are most indicative of the reaction mechanisms involved and are discussed below.

H_2-NO_2 Flame Structure

Measurements of the composition of stable and unstable species and temperature in laminar, premixed, flat flames of H_2-NO_2-Ar have been made and compared to the structure calculated with a flame code including detailed chemical kinetics (ref. 9). No previous detailed flame structure measurements and chemical kinetic modeling of this flame have been presented. Similar measurements and calculations are reported for a companion H_2-O_2-Ar flame in order to provide a comparison to a previously well characterized flame. We have modeled these flame measurements using the 272 step reaction mechanism with the carbon species removed. The resulting 87 step mechanism gives good agreement to the experimental data as shown in Figure 2.

In contrast to the H_2O-O_2-Ar flame, the rate and sensitivity calculations for H_2, NO_2, H_2O and OH in the H_2-NO_2-Ar flame show that species net reaction rates are usually dominated by a single reaction. Almost all of the H_2 consumption and H_2O formation is by $OH+H_2=H_2O+H$. The consumption of NO_2 and formation of NO is almost entirely by $NO_2+H=NO+OH$. The sum of these two reactions gives the global reaction of the flame $H_2+NO_2=NO+H_2O$. There is some formation of O_2 early in the flame by $NO_2+O=NO+O_2$ followed by O_2 consumption by $O_2+H=O+OH$. The OH is a balance of formation by $NO_2+H=NO+OH$ and consumption by $OH+H_2=H_2O+H$.

The reactions with greatest negative sensitivity for H_2 and NO_2 have the highest positive sensitivity for NO and H_2O. The reactions with the largest positive sensitivity for H_2 and NO_2 likewise have the largest negative sensitivity for NO and H_2O. The OH is primarily sensitive to its major formation and consumption reactions.

The importance of the reaction $H_2+NO_2=HNO_2+H$ to the H_2-NO_2-Ar flame mechanism is observed in the sensitivity and analysis for H_2, NO_2, NO, H_2O and OH. This reaction provides the most important initiation step. It also has a significant effect on the OH profile by producing H early in the flame and promoting the formation of OH by $NO_2+H=NO+OH$. The HNO_2 is subsequently consumed by several reactions. Using a mechanism that contains only the three reactions

$$NO_2 + H = NO + OH$$
$$OH + H_2 = H_2O + H$$
$$H_2 + NO_2 = HNO_2 + H$$

gives a flame model that compares to within 5% of the model using the entire reaction mechanism.

<u>C_2H_2-NO_2 Flame Structure</u>

Volponi and Branch (ref. 9) studied C_2H_2 reacting with NO_2 in an argon diluent at a pressure of 25 torr. We modeled this flame using the 272 step reaction mechanism and the measured temperature profile. The modeling results using this mechanism are close to those Volponi and Branch obtained using the full, 331-reaction mechanism from which the 272-reaction mechanism was derived. This indicates that modeling results are not significantly affected using the smaller mechanism.

Measured and modeled mole fraction profiles for major species are shown in Figure 3. Discrepancies can be seen near the burner surface, as the modeling overpredicts the surface mole fractions of unreacted species and underpredicts the surface mole fraction of product species. Agreement is good, however, in the general trends shown in the profiles, and in the final mole fractions obtained in the flame. The modeling was used to find the principal reactions involved in each specie's production/consumption. The principal reaction consuming C_2H_2 is $C_2H_2+OH=C_2H+H_2O$; the principal reaction consuming NO_2 is $NO_2+H=NO+OH$; the principal reaction producing NO is $NO_2+H=NO+OH$; the principal reaction producing O_2 is $2NO_2=2NO+O_2$; the principal reaction producing CO_2 is $NO_2+CO=NO+CO_2$, and the principal reaction producing H_2O is $OH+C_2H_2=C_2H+H_2O$. The importance of radicals in breaking down the unreacted species is evident.

Comparisons were also made between modeled and measured mole fractions for the radical species OH and CN. There were discrepancies in the calculated and measured trends for these species. The principal reaction involving OH production is $NO_2+N=NO+OH$, and the principal reaction involving CN production is $HCN+OH=CN+H_2O$, and the principal reaction involving CN production is $HCN+OH=CN+H_2O$.

Volponi and Branch (ref. 3) also modeled C_2H_2 reacting with O_2 with Argon gas as a diluent at a pressure of 25 torr. We modeled this flame using the 272 step mechanism and the measured temperature profile. The modeling's accuracy was on a par with what was obtained for the CH_4/N_2O flame. Modeling was generally in good agreement with experimental data for major species concentrations in the flame, with the exception of H_2O, whose concentration was slightly underpredicted. Modeling and experiments agreed in the general trends for the concentration of radical species OH and CH, but modeling overpredicted the peak concentrations of both species by a factor of two. As with the CH_4/NO_2 flame, our modeling results compared well with those Volponi and Branch obtained using the 331-reaction mechanism.

A.2.3 FLAMES SUPPORTED BY NO AS OXIDIZER

Zabarnick (ref. 6) studied a $CH_4/NO/O_2$ flame at 63 torr, using LIF to measure temperature and stable and radical species concentrations. This flame was modeled using the measured temperature profile and the 272 step mechanism.

The measured NO concentration profile showed a more pronounced drop-off to a steady-state value than modeling predicted. Also, the final calculated value of NO in the flame is 50% higher than what was measured; NO was the only stable species Zabarnick performed measurements on in this work.

Modeling and experimental results were compared for radical species. The predicted peak concentration of CN leads the experimentally measured peak by about 1 mm. The predicted OH concentration showed a drop-off late in the flame that was not detected experimentally. The predicted NH peak led the measured peak by about .5 mm. The predicted CH peak led the measured peak by about 1 mm also. Note that modeling now leads the experimental data for the location of peak radical concentrations, while for the CH_4/N_2O flame also measured by Zabarnick (ref. 6) modeling predictions generally lagged the experimental data.

A.2.4 BURNING VELOCITY OF FUEL/NO_x LAMINAR PREMIXED FLAMES

The 272 step reaction mechanism was used to model the burning of free-standing flames supported by N_2O and NO_2, and the modeled flame speed was compared to the experimental results obtained by Parker and Wolfhard (ref. 12) using the bunsen burner technique (Table 2). Also shown are the burning velocities obtained with the Miller and Bowman (ref.13) mechanism without the modifications discussed in the present investigation. The results indicate that generally good agreement is obtained between the modeling and the experimental data and that the 272 step mechanism gives better results than earlier mechanisms. The burning velocity of the flames with N_2O are significantly higher than those with NO_2 as oxidizer. Two of the calculations are discussed below in more detail in order to indicate the importance of fuel and oxidizer decomposition reactions in flame propagation.

Table 1 gives the calculated and measured results for the burning rate of a CH_4/N_2O flame. The calculated flame velocity is 90 cm/sec, very close to the measured velocity of 105 cm/sec. In addition, for this flame we were able to perform analysis on what reactions contribute most strongly to a given specie's production/consumption. It was found that the major reactions leading to the decomposition of CH_4 are the following, in decreasing order of their rate of CH_4 consumption:

$$CH_4 + H = CH_3 + H_2$$
$$CH_4 + OH = CH_3 + H_2O$$
$$CH_4 + O = CH_3 + OH$$

The major reactions leading to the breaking down of N_2O were found to be, in decreasing order of the amount of N_2O they consume:

$$N_2O + H = H_2 + OH$$
$$N_2O + M = N_2O + M$$

The importance of the radicals H, OH and O are clearly evident in the propagation of this flame.

A free-standing C_2H_4 flame at a pressure of 0.1 atm was modeled and the calculated flame speed was compared to that measured by Parker and Wolfhard (ref. 10). The results are included in Table 2, and as can be seen, the agreement is excellent for this flame. It was difficult to obtain a converged solution modeling many NO_2-supported flames, so there are not more cases reported at this time. It is possible that the larger mechanism used to model this flame aided in obtaining better agreement with experimental data than was obtained in several of the cases of N_2O-supported flames. More cases would need to be run, however, to draw conclusions on the relative ability of the two mechanisms to model free-standing flames supported by NO_2 and N_2O.

Modeling results for this flame showed that the top four reactions contributing to the decomposition of C_2H_4 in the flame were the following:

$$C_2H_4 + OH = C_2H_3 + H_2O$$
$$C_2H_4 + M = C_2H_2 + H_2 + M$$
$$C_2H_4 + H = C_2H_3 + H_2$$
$$C_2H_4 + O = CH_3 + HCO$$

The top four reactions leading to the decomposition of NO_2 were found to be:

$$NO_2 + N = NO + OH$$
$$NO_2 + CO = NO + CO_2$$
$$NO_2 + M = NO + O + M$$
$$NO_2 + OH = HO_2 + NO$$

Initiation of the chemistry in these flames can be seen to be closely tied to reactions producing radical species.

A.2.5 SUMMARY AND CONCLUSIONS

We have completed detailed comparisons of calculations and measurements of the structure and burning velocity of fuel/NO_x mixtures using a 272 step reaction mechanism. The comparison between the calculated flame structure and the experimental flame structure for stable species was found to be very good for fuel/N_2O flames and good for fuel/NO_2 flames. The concentration profiles for radical species were found to be generally well represented qualitatively but not well represented quantitatively. It was concluded that, despite some remaining difficulties with the reaction mechanism, it appeared to be reliable

in describing the overall combustion behavior of a wide range of fuel and oxidizer mixtures.

The most important reactions of the oxidizer (N_2O or NO_2) are with H atoms and, to a lesser extent, with CO. Reaction of either oxidizer with H is a chain propagating reaction, in contrast with the chain branching reaction of H with O_2 which is of equal importance in fuel oxidation by O_2. In addition, the reaction of NO_2 with H is slower than N_2O with H. Finally, the reaction of N_2O with CO can be significant both in consumption of CO and formation of CO_2. This situation is again in contrast with the oxidation chemistry of systems by O_2 in which the conversion of CO to CO_2 is almost entirely be reaction of CO with OH. The difference between the use of N_2O or NO_2 as oxidizer is that the former produces primarily N_2 while the latter produces NO. The subsequent slow reduction of NO to N_2, even when it is thermodynamically favored, accounts for the most striking difference between the two oxidizers. The most important effects of the oxidizer, therefore, are that the nitrogen oxides are less effective chain carriers and lead to slower reaction rates compared to O_2.

The oxidation reactions of CH_4 in the presence of NO_x is generally similar to the oxidation by O_2. Chain propagating and branching reactions lead to the formation of H, O and OH and these species progressively abstract hydrogen and partially oxidize CH_3 to CH_2O. The CH_2O is then converted largely to CO through the intermediate HCO. Subsequent oxidation of CO to CO_2 is by reaction with NO_x of OH as mentioned above. If the fuel is CH_2O instead of CH_4, the latter stages of this chain become dominant. If the fuel is C_2H_2 instead of CH_4, then reactions of CH_2 become more important and CH_2O becomes less important. Rate constants for the reactions involved in the hydrocarbon chemistry derived from previous studies are generally successful in the description of the transformation of CH_4 to CO.

The third major aspect of fuel/NO_x flame chemistry is the interaction of H, C and N containing species. Reaction of CH_i species with NO to form HCN and subsequent reaction of HCN, CN or NCO with NO lead to the conversion of NO to N_2. This process is obviously of most importance when NO_2 or NO is the oxidizer rather than when N_2O is oxidizer, since in the latter case N_2 is formed directly. This scheme also shows the essential features of the oxidation process in the case where HCN is formed as a fuel during the decomposition of the energetic solid.

A.3 REFERENCES

1. Korobeinichev, O.P., L.V. Kuibida and V.Z. Madirbaev, Combustion, Explosion, and Shock Waves 20, pp. 282-285, (1984).

2. Korobeinichev, O.P., A.G. Tereschenko, A.A. Schvartsberg, G.A. Makhov and A.E. Zabolotny, Flame Structure 1, edited by O.P. Korobeinichev, pp. 262-267, (1991).

3. Volponi, J.V., and M.C. Branch, "Flame Structure of C_2H_2-O_2-Ar and C_2H_2-NO_2-Ar Laminar Premixed Flames," 24th Symposium (International) on Combustion, in press.

4. Kee, R.J., J.F. Grcar, M.D. Smooke and J.A. Miller, "A Fortran Program for Modeling Steady Laminar One-Dimensional Premixed Flames," Report SAND 85-8240, Sandia National Laboratories, Livermore, (1985).

5. Habeebullah, M.B., F.N. Alasfour and M.C. Branch, 23rd Symposium (International) on Combustion, The Combustion Institute, Pittsburgh, pp. 371-378, (1991).

6. Zabarnick, S., Combustion Science and Technology, 83, pp. 115-134, (1992).

7. Vandooren, J., P.J. Tiggelen and M.C. Branch, "Measurements of the Structure of $CH_4/N_2O/Ar$ and $CH_4/O_2/Ar$ Flames by Molecular Beam Sampling and Mass Spectrometric Analysis," Combustion and Flame, in press.

8. Dindi, H., H.M. Tsai and M.C. Branch, Combustion and Flame, 87, pp. 13-20, (1991).

9. Volponi, J.V., and M.C. Branch, "Flame Structure of $H_2/NO_2/Ar$ Laminar Premixed Flames," Paper No. WSS/CI 90-02, Western States Section-Combustion Institute, October 1990. Also, Combustion Science and Technology, under review.

10. Branch, M.C., A. Alfarayedhi, M. Sadeqi and P.J. Van Tiggelen, Combustion and Flame, 83, pp. 228-239, (1991).

11. Zabarnick, S., Combustion and Flame, 85, pp. 27-50, (1991).

12. Parker, W.G and H.G. Wolfhard, 4th Symposium (International) on Combustion, Williams and Wilkins, Baltimore, pp. 420-428, (1953).

13. Miller, J.A., and C.T. Bowman, Progress in Energy and Combustion Science, 15, pp. 287-338, (1989).

A.4 RECENT PAPERS AND PRESENTATIONS FROM THIS AND PREVIOUS AFOSR SUPPORT

1. M.B. Habeebullah, F.N. Alasfour and M.C. Branch, "Structure and Kinetics of CH_4/N_2O Flames," *23rd Symposium (International) on Combustion*, the Combustion Institute, Pittsburgh, pp. 371-378, 1991.

2. H.Dindi, H.M. Tsai and M.C. Branch, "Combustion Mechanisms of Carbon Monoxide-Nitrous Oxide Flames," *Combustion and Flame*, 87, pp. 13-20, 1991.

3. M.C. Branch and H. Dindi, "Measurements and Chemical Kinetic Simulation of the Structure of Model Propellant Flames," *Proceedings of the AFOSR Contractors' Meeting on Propulsion*, University of Colorado, pp. 165-168, 1991.

4. J. Vandooren, M.C. Branch, and P.L. Van Tiggelen, "Comparisons of the Structure of Stoichiometric CH_4-N_2O-Ar and CH_4-O_2-Ar Flames by Molecular Beam Sampling and Mass Spectrometric Analysis," *Combustion and Flame*, 90, pp. 247-258, 1992.

5. M.C. Branch, "Structure and Chemical Kinetics of Flames Supported by Nitrogen Oxides," *AFOSR Contractors' Meeting*, University of California, San Diego, pp. 102-106, 1992.

6. M.C. Branch, "Structure ad Chemical Kinetics of Flames Supported by Nitrogen Oxides," *Pure and Applied Chemistry*, 65, No. 2, pp. 277-283, 1993.

7. J.V. Volponi and M.C. Branch, "Flame Structure of C_2H_2-O_2-Ar and C_2H_2-NO_2-Ar Laminar Premixed Flames," *24th Symposium (International) on Combustion*, The Combustion Institute, Pittsburgh, in press.

8. J.W. Volponi and M.C. Branch, "Flame Structure of H_2O-NO_2-Ar Laminar Premixed Flames," Paper No. WSS/CI 90-02, *Western States Section/Combustion Institute*, October 1990. Also, *International Colloquium on Dynamics of Explosions and Reactive Systems*, under review.

A.5 PERSONNEL

1. Greg Fiechtner, Postdoctoral Research Associate, University of Colorado, Boulder.
2. Hai-Ming Tsai, Ph.D. Candidate, University of Colorado, Boulder.
3. Joseph Cor, Ph.D. Candidate, University of Colorado, Boulder.
4. Andy Wilson, Undergraduate Research Affiliate, University of Colorado, Boulder.
5. Matthew Fuller, Undergraduate Research Affiliate, University of Colorado, Boulder.

TABLE 1. Rate constants used in the present 272 Step Reaction Mechanism which differ from those of Volponi and Branch (Ref. 3). Units are mole, cm^3, sec, K, and Cal/mole.

Reaction	A	n	Ea
$N_2O+OH=N_2+HO_2$	1.00e13	0	10000
$N_2O+H=N_2+OH$	1.50e14	0	15090
N_2O+M+N_2+O+M	4.90e15	0	57500
$N_2O+O=N_2+O_2$	7.00e14	0	28200
$N_2O+O=2NO$	5.60e14	0	28200
$CO+N_2O=CO_2+NO$	2.00e12	0	17300

TABLE 2. Comparison of measured and calculated flame speed of fuel/NO_x mixtures[a].

REACTANTS	MEASURED[b]	CALCULATED	
		M/B[c]	This Work[d]
H_2/N_2O	300	227	240
CH_4/N_2O	105	76.2	90
C_2H_2/N_2O	160	128	150
C_2H_4/N_2O	110	94	102
C_2H_4/NO_2	62.5	61	61

(a) All flame speeds given in cm/sec at 0.10 atm and for a stoichiometric mixture.
(b) Parker & Wolfhard (Ref. 12).
(c) Calculation using mechanism of Miller & Bowman (Ref. 13).
(d) Calculation using the present 272 step mechanism.

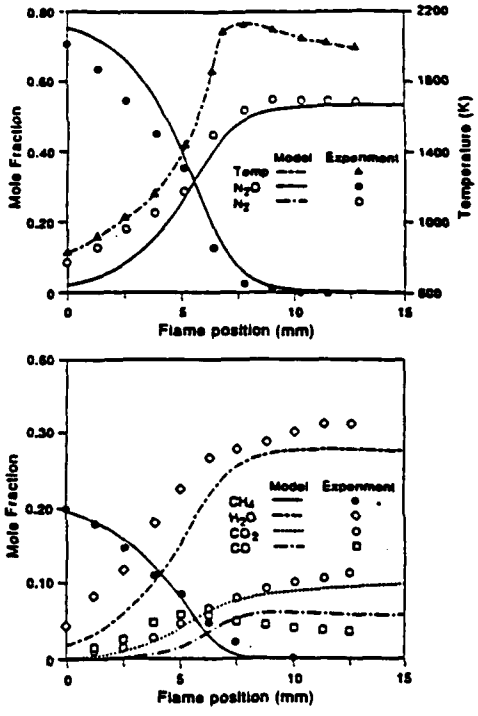

Figure 1. Comparison of CH_4/N_2O flame structure data of Habeebullah et al. (Ref. 5) to calculations of flame structure using 272 step reaction mechanism.

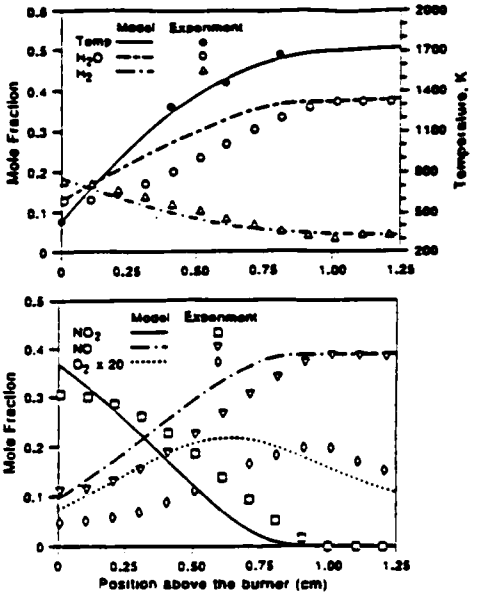

Figure 2. Comparison of H_2/NO_2 flame structure data of Volponi and Branch (Ref. 9) to calculations of Flame Structure Using 272 step reaction mechanism.

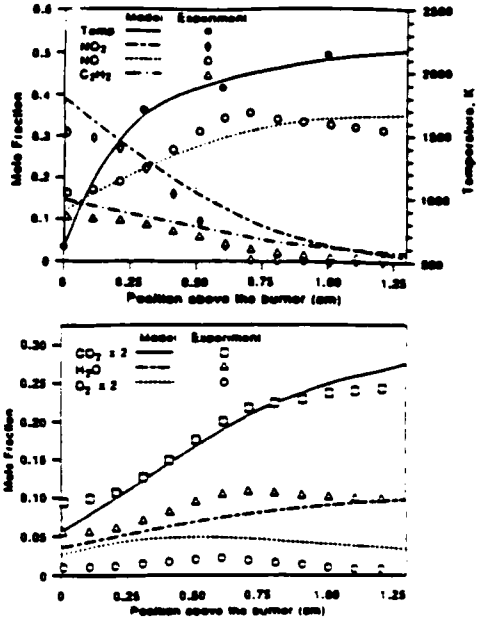

Figure 3. Comparison of C_2H_2/NO_2 flame structure data of Volponi and Branch (Ref. 3) to calculations of flame structure using 272 step reaction mechanism.

B. FUNDAMENTAL STUDIES OF ROCKET COMBUSTION INSTABILITY

B.1 RESEARCH OBJECTIVES

Rocket engine manufacturers rely heavily on empirical and actual test data during the design stage of rocket engines in order to prevent the occurrence of instabilities during flight operation. This is clearly an expensive approach. Thus, the long term objective of our research is to develop predictive models that will help rocket designers build high performance, stable liquid rocket engines.

A complex interaction of several processes such as atomization of the primary fuel jet, secondary atomization of the resulting drops, vaporization, mixing and combustion are responsible for liquid rocket engine instability. Since atomization is the first mechanism in the chain of events leading to eventual combustion and possibly combustion instability, our near term objective is to understand the influence of atomization on the stability properties of rocket engines. The focus of our work is to elucidate and model the response of atomization under controlled modulated conditions.

B.2 BACKGROUND

Combustion instability that is characterized by large amplitude combustion chamber pressure oscillations is a commonly observed feature in many liquid propelled rocket engines. Severe engine damage could result due to mechanical failure and/or enhanced heat transfer to the chamber. Liquid fuel injected into a rocket engine combustion chamber undergoes a sequence of processes prior to exiting the chamber in the form of products of combustion. A typical scenario leading to combustion instability is as follows: an initial chamber pressure disturbance induces fluctuations in atomization rate. This results in variation of propellant droplet size distribution, which affects vaporization, mixing and reaction rates, inducing fluctuations in the engine burning rate. This process can feed energy back into the pressure field, thus closing the loop. If proper phase relationship is achieved during these processes, amplification of initial disturbances can occur, leading to combustion instability. Integration of all the physical processes involved into a comprehensive model of engine stability is not probable, unless each process is well understood.

Injectors in liquid rocket engines are exposed to relatively high amplitude pressure and velocity field oscillations (acoustic waves). These oscillations have a pronounced effect on the atomization of liquid propellant. Sufficient evidence from past work and our present research reveals that the structure and characteristics of atomization under unsteady conditions (as would occur during a combustion instability) deviate considerably from atomization behavior under steady conditions. Thus, the dynamic behavior of liquid propellant atomization is of major importance, especially when atomization produces very small droplets.

Miesse (1955) showed that significant acoustic interactions can be achieved between a low speed jet and local, high amplitude sound fields. Reba and Brosilow (1960) conducted the first experiment on liquid jet behavior perturbed by a longitudinal acoustic wave created by a siren (their work is also reported by Torda and Schmidt, 1964). Buffum and Williams (1967) investigated the behavior of a liquid jet subject to a transverse standing acoustic field. They studied the periodic oscillations of the liquid jet position in space and argued that this phenomenon might explain combustion instability in liquid rocket engines with impinging jet type injectors. Jet oscillatory deviations cause fluctuations in impingement point and geometrical injection parameters, which can induce variations in the atomization rate and pattern. Their

results showed a strong correlation between the acoustic field and the jet behavior for forcing amplitudes of 160 dB and frequencies up to 500 Hz.

Heidmann (1965) studied acoustic field and jet interaction in a two-dimensional circular combustor. He found a strong correlation between the acoustic field and the oscillatory jet breakup behavior. Ingebo (1966) studied the behavior of liquid jet atomization perturbed by longitudinal acoustic waves. A siren periodically obstructed the chamber exit and created longitudinal acoustic perturbations. Streak photography showed reversal of the gas flow during instability. High speed photography provided the first measurement of drop size distribution under unsteady and hot environment. He showed that under resonant conditions, atomization and vaporization rates are significantly enhanced. The jet breakup length was one sixth compared with the unforced case. Much finer droplet size was obtained (62 microns in resonant forcing conditions and 217 microns for unforced cases). The length for complete vaporization decreased from ~50 cm to 5 cm. More recently, Lecourt and Foucaud (1987) studied the stability of several injectors using the forcing method developed by Ingebo. Due to extreme operating conditions (1000 psia), only pressure-time traces were recorded.

Heidmann and Groeneweg (1969) studied the transfer function between pressure oscillations and atomization rate. They argued that if the in-phase transfer function is positive, unstable combustion might occur. The justification for this approach comes from the Rayleigh criterion. Different types of transverse acoustic oscillations (travelling, standing, radial transverse mode and vortex mode, characterized by a steady tangential velocity component) were investigated experimentally and analytically. They found that variations in the peak values of the response factors are caused by the velocity sensitivity of the atomization process, and a velocity perturbation, in-phase with pressure, elevated the peak value and is destabilizing to a combustion system. However, an out-of-phase velocity perturbation reduced the peak value of the response factor and is stabilizing. They predicted that potentially the maximum average response for the traveling mode is larger than for either the standing or radial modes. Both their analytical and experimental results indicated that a steady vortex velocity had an amplifying effect and increased the peak value of the response factor by an order of magnitude.

Overall, very little is known about the dynamics of atomization under modulated conditions. Current interest in combustion instabilities of liquid rocket engines and the advent of modern diagnostics has initiated our study of atomization behavior under oscillatory environment. In our work external forcing is used to simulate combustion induced pressure and velocity fluctuations. The advantage is a complete control over frequency, and amplitude, so that linear and nonlinear forcing regimes can be investigated. Our study focuses on the phase and amplitude relationship between forcing and atomization response. Although these quantities have been shown to be important in theoretical studies on the possible coupling between atomization and acoustic waves leading to combustion instability, they have never been measured. This knowledge can lead to the use of linear stability theory to clarify the role of atomization in high frequency combustion instability.

B.3 DESCRIPTION OF EXPERIMENTAL FACILITY

As one of the objectives of this research program is to provide useful atomization information for the design of actual injectors, it is important to give special attention to similarity parameters. Moreover, it is extremely difficult to model a real rocket engine because of the severe conditions encountered in an actual combustion chamber. High pressure and intense heat transfer rates precludes accurate measurement of quantities such as pressure, temperature and droplet size distribution. Propellants used in the rocket

industry are usually toxic and hypergolic. The approach adopted is to identify dimensionless numbers, which govern atomization and try to maintain them, or at least operate in the proper range. Four dimensionless numbers, liquid jet Reynolds number

$$Re_l = \frac{\rho_l V_l d_o}{\mu_l} ,$$

Weber number based on gas phase properties

$$We_g = \frac{\rho_g (V_g - V_l)^2 d_o}{\sigma_l} ,$$

μ_l/μ_g, and ρ_l/ρ_g, are used to characterize atomization. Here, the symbols μ and ρ represent dynamic viscosity and density. The subscripts l and g indicate liquid and gas. However, the definition of the quantities which are chosen to calculate the Reynolds and Weber numbers varies in the literature.

The turbulence level in the liquid phase, as the jet emerges from the nozzle is important because it characterizes the amplitude of the disturbances on the jet surface, which are likely to be amplified by dynamic interactions with the surrounding gas. This justifies our definition of the Reynolds number. The Weber number based on gas phase properties takes into account aerodynamic forces, the main mechanism for jet breakup and atomization at high velocities. Although no single mechanism can explain the entire process of atomization, aerodynamic interactions between the liquid jet and the surrounding gas provide the main destabilizing agent (Reitz and Bracco, 1986).

A survey of studies on coaxial injectors has been completed. The operating range of relevant results is reported in a Re_l - We_g diagram in Figure 1. The two horizontal lines correspond to theoretical results from Ranz (1958) and Miesse (1955), who predicted that atomization regime lies beyond a critical We_g. Our approach is to operate in the atomization regime and come as close as possible to the configuration under simulation by a proper choice of simulants.

B.3.1 Simulation Selection

Since real atomizer injection velocities are very high, they cannot be increased to maintain similarity. A survey of different propellant combinations revealed that the best which can be done is to maintain the value of liquid and gas velocity. In order to maintain geometrical similarity, we have retained the inner post diameter (Figure 2). Therefore, the dimensionless numbers indicate that the simulant selection is governed by the following two equations.

$$\left(\frac{\rho_l}{\mu_l}\right)_{actual} = \left(\frac{\rho_l}{\mu_l}\right)_{model}$$

$$\left(\frac{\rho_g}{\sigma_l}\right)_{actual} = \left(\frac{\rho_g}{\sigma_l}\right)_{model}$$

Tables 1 and 2 show the values of ρ_l/μ_l and ρ_g/σ_l for different combinations for both hot and cold run simulations of LO_x/GH_2 rocket propellants. For cold flow testing, the combination Freon 113, R13B seems adequate, if atomization data on LO_x/GH_2 is to be obtained. For hot flow tests, one sees that for all simulants (hydrogen peroxide, ethanol) the value of ρ_l/μ_l falls short by a factor of at least 2.

In our case, we chose to use a combination of water and air mixed with refrigerant for cold flow runs. For experiments with combustion, the ethanol/air mixed with oxygen combination has been selected.

B.3.2 Combustor Design

The size of the combustor chamber has to be chosen carefully to ensure almost complete combustion before the nozzle exit. In particular, considerations using parameters such as L^* or t_w helped us in our task. The quantity L^* is a ratio of chamber volume to throat area. Values of L^* must be chosen in accordance with the fuel-oxidizer choice. The fluid residence time in the chamber is denoted by t_w. Also, the selected excitation system places a bound on the size of the chamber, because large amplitude modulations are possible only if the chamber volume is small enough.

The combustion chamber design is shown in Figure 3. The uni-element coaxial combustor has transverse dimensions of 5 cm x 5 cm. The chamber is designed to withstand a pressure of 10 atm absolute. This limitation comes from the quartz windows (1.25 cm thick). The chamber length can be varied from 28 to 43 cm by moving the exit nozzle location. The adjustable length allows for the study of various combustion efficiencies and longitudinal acoustic modes. The length of the chamber dictates the residence time of the reactants and hence the amount consumed, or in essence the combustion efficiency. Two quartz windows, 25 x 5 cm, on opposite sides of the chamber provide full optical access from the injection plane to 25 cm downstream. The operating pressure of the chamber for given fuel and oxidizer mass flow rates can be varied by using exit nozzles of different throat area. The chamber is mounted vertically to eliminate liquid accumulation during cold flow tests. The injector head is made of a 5 x 5 x 7 cm stainless steel block, as shown in Figure 2. The injector head can easily be modified to accommodate other types of atomizers such as an impinging jet. The center post of the injector is machined to allow for smooth reduction of liquid fluid passage area. The mounting of the center post can be adjusted to achieve the desired recess relative to the injection plane. Center posts of different design and diameter can be mounted into the injector block. The injector used in this study has a center post with inside diameter of 1 mm with a 4 mm width of the surrounding annulus.

B.3.3 Excitation Method

Acoustic compression drivers are used to excite transverse modes in the combustion chamber. The experimental configuration is shown in Figure 4. This kind of perturbation is chosen because, in many high frequency combustion instability cases, the coupling between combustion and chamber transverse acoustic modes have been recorded. The use of acoustic excitation devices in studies in the field of active control of combustion instability has proved to be successful. In particular, very high pressure excitation levels can be obtained.

Most acoustic drivers operate adequately in the frequency range from 1000 Hz to 6000 Hz. Moreover, many high frequency combustion instabilities are encountered in this range. Hence, the excitation frequency domain for transverse excitation is chosen as above. This sets the chamber transverse dimension to under 5 cm. It is also desirable to excite the chamber at a frequency different from any of its characteristic frequencies, in order to avoid resonance. Thus, we can exercise complete control on the

amplitude of modulation. High forcing pressure amplitudes can be obtained by tuning the length of the ducts connecting the compression chambers to the combustion chamber.

B.4 DIAGNOSTIC TECHNIQUES

Diagnostic techniques aimed at studying this configuration are under development. In particular, the time variation of quantities such as atomization rate, jet breakup length, length for complete atomization, under forcing and non-forcing conditions are of interest. Large and small scale fluid mechanical fluctuations and their phase with respect to external excitation are also important in better understanding the dynamic behavior of atomization. The task is difficult because the frequency range of interest is above 1000 Hz. Currently, phase locked, back-lighted photography and Schlieren are used. Diagnostic systems like the ones in Figures 5 and 6 can give access to the aforementioned interesting quantities. The signal from the acoustic drivers is used to periodically trigger a light source. An optical arrangement focuses the light onto a region of the atomizing jet. The resulting image is captured by a continuous high speed camera. Phase averaging is then used to minimize cycle-to-cycle variations. The images are then processed to extract jet breakup length and characteristic time for complete atomization. By shifting the phase of the light trigger with respect to the excitation signal, phase sensitive images of the atomizing jet are obtained.

Currently, the response of the chamber pressure and localized heat release in the combusting region to an acoustic perturbation is under investigation. In particular, the amplitude and phase of the response relative to the perturbation is being analyzed. A piezoelectric transducer mounted on the chamber wall measures the chamber pressure response. This type of transducer is capable of measuring high frequency and low amplitude acoustic waves. The localized heat release is measured by collecting the light emitted by C2 radicals, which are only present in the high temperature combusting regions of the flow. The measurement is local in the sense that an optical system only gathers light from a very small region in the combustion region. The emitted light is collected and focused onto a photomultiplier tube for signal generation. In this manner, a relative measure of the localized heat release can be obtained for comparison between excited and unexcited conditions.

In addition, laser back scattering and extinction diagnostic systems are under development, as shown in Figure 7. These systems are capable of measuring the atomization response to an imposed perturbation. The idea is to focus a He-Ne laser beam into the initial atomizing region near the inner post tip, the scattered light is then collected by a series of PMT detectors and the extinction of the laser beam is measured by a photo diode. The intensity of the laser beam received by the photo diode is directly proportional to the amount of fluid which has passed through it. Spectral analysis of the signals can then give information concerning the modification of frequency content of the atomization process due to acoustic perturbations.

B.5 RESULTS

B.5.1 Cold Flow Results

A series of pressure measurements inside the chamber have been conducted in order to obtain the fluctuating pressure and velocity field generated by the excitation system. The measurements indicate that transverse acoustic field strengths of up to 156 dB, and acoustic velocity fluctuations of up to 4.2 m/s at the injector location can be produced.

A numerical code using linear acoustic equations has been developed to model the pressure field in the test section. The equations are solved using a second order accurate finite difference scheme. Input includes the acoustic driver boundary conditions and a temperature map of the system to account for the speed of sound distribution. Output includes the acoustic modes for the system, and resulting pressure and velocity fields. The code will be enhanced to include flow within the chamber to better model real conditions.

A set of experiments has been carried out to determine the effect of acoustic forcing on the global behavior of the fuel spray. These measurements are difficult due to the accumulation of fluid on the windows of the chamber. The results indicate that under out-of-phase forcing conditions, there is an increase in the volume of fuel droplets drawn into the recirculating region at the top of the chamber. Visually, the level of fluid accumulated on the window rises with excitation. Further experiments are planned to elucidate the physical phenomenon and obtain precise quantitative results.

B.5.2 Hot Flow Results

The combustion/excitation system has been improved and made ready for experimentation. Smooth reliable combustion, as well as integration with the excitation system has been obtained. The operating limits involving reactant parameters and chamber geometrical settings have been explored. In addition, the diagnostic Schlieren imaging technique has been refined to generate high quality(contrast) imaging of the flow during hot runs, as shown in Figure 8.

Recent experimentation has been conducted to determine the effect of equivalence ratio and excitation amplitude upon the time variation of the chamber pressure between forced and unforced conditions. The gas phase and liquid phase velocities were held constant at 92 m/s and 15 m/s, respectively. The equivalence ratio was varied by the addition of pure oxygen to the gas phase resulting in a range from 3.8 to 7.4 . These procedures were carried out in order to keep the atomization characteristics of the system constant. The enrichment of the gas phase with oxygen increased the gas phase velocity very little. Moreover, the aerodynamic properties of oxygen are essentially similar to air. Thus, atomization parameters including Weber number and density ratio were held relatively constant. However, the static chamber pressure varied with equivalence ratio. This was caused by the use of the same size chamber exit nozzle for all the experiments. A variety of exit nozzles are under construction in order to decouple the chamber pressure from equivalence ratio. As an example, for an experiment with an equivalence ratio near one, which is a high heat release and hence high chamber pressure case, a larger exit nozzle will be used to reduce the chamber pressure so that it will remain constant.

Unexcited chamber pressure recordings for equivalence ratios of 7.4 and 3.8 are shown in Figures 9 and 13, respectively. The power spectra of these signals, shown in Figures 10 and 14, indicate the presence of three frequency ranges. The first range is centered at 200 Hz and the other two ranges are centered at 1250 Hz and 2500 Hz. There is a slight increasing shift of these ranges as the equivalence ratio is reduced(approaches one). This is probably caused by the fact that as stoichiometric conditions are approached, the chamber experiences higher temperatures and thus higher sound speeds, and hence increased oscillation frequency.

The acoustic compression drivers were tuned to excite the chamber at 2950 Hz. This frequency was chosen because it corresponds to a large amplitude pressure fluctuation in the chamber (determined experimentally), and it is in the high frequency (screeching) range. Chamber pressure records under forced conditions, for equivalence ratios of 7.4 and 3.8 are shown in Figures 11 and 15, respectively. The power

spectra of these signals, shown in Figures 12 and 16, indicate a peak at the excitation frequency. This is expected because the combustion chamber, excitation system, and pressure transducer are in a closed system. The interesting result is that the observed peak at the excitation frequency increases as the equivalence ratio is decreased. The peak power at the excitation frequency versus equivalence ratio is displayed in Figure 17. This result is biased by the fact that the static chamber pressure also increased with decreasing equivalence ratio. As stated earlier, the elimination of this bias is underway.

The effect of excitation amplitude for a fixed equivalence ratio of 3.8, holding all other parameters constant, was examined. As shown in Figure 18, the peak power at the excitation frequency increases as the excitation amplitude is increased. Again, this was expected because the pressure transducer and excitation system are in a closed system.

Currently, work is under way to determine the effect of gas phase velocity, equivalence ratio, excitation frequency, chamber length, and injector post recess upon the time variation of chamber pressure and localized heat release (C2 emission) between forced and unforced conditions. Schlierien images are being acquired to analyze the fluid mechanical response to excitation, i.e (jet breakup length, length for complete atomization, vortical structure,...etc). The analysis includes an examination of the frequency content (power spectra) of the measured signals to determine if the acoustic forcing frequency can drive the physical process under investigation. The phase and amplitude response of the signals relative to the perturbation will also be obtained. This information is a direct measure of the (n,τ) parameters applied to (n,τ) correlations commonly used in industry to predict instability behavior. In addition, auto- and cross-correlations of these signals will be acquired to determine the periodicity and similarity of the measured signals and perturbation.

B.6 FUTURE WORK

Laser backscattering and extinction experiments are planned to obtain real time data on spray fluctuations in order to measure the frequency response of atomization to acoustic perturbation. Furthermore, a Phase Doppler system is under development in order to measure the fluctuation in drop size and drop velocity in the atomizing region. Thus, this system will provide precise quantitative measurements of real physical atomization parameters and give a more clear understanding of atomization response.

In addition, an image processing system has been acquired. This system will generate sharp, detailed images of the spray and flow structure. Phase averaging can then provide statistically reliable quantitative information concerning fluid mechanical response.

B.7 REFERENCES

1. Buffum, F.G., and Willams, F.A., "The response of a Turbulent Jet to Transverse Acoustic Fields," *Proceedings of the 1967 Heat Transfer and Fluid Mechanics Institute*, P.A. Libby, D.B. Olfe and C.W. Van Atta, Eds., Stanford University Press, 1967, pp. 247-276.

2. Ghafourian, A., Mahalingam, S., Dindi, H., and Daily, J.W., "A Review of Atomization in Liquid Rocket Engines," *AIAA 29th Aerospace Sciences Meeting*, AIAA 91-083, Reno, NV, Jan. 7-10, 1991.

3. Heidmann, M.F., "Oxygen-Jet Behavior During Combustion Instability in a Two-Dimensional

Combustor," *NASA TN D-2725*, 1965.

4. Heidmann, M.F., and Groegneweg, J.F., "Analysis of the Dynamic Response of Liquid Jet Atomization to Acoustic Oscillations," *NASA TN D-5339*, 1969.

5. Ingebo, R.D., "Atomization of Ethanol Jets in a Combustor With Oscillatory Combustion-Gas Flow," *NASA TN D-3513*, 1966.

6. Lecourt, R., and Foucaud, R., "Experiments on Stability of Liquid Propellant Rocket Motors," *23rd AIAA Propulsion Conference*, San Diego, CA, 29 June-2 July, 1987.

7. Miesse, C.C., "Correlation of Experimental Data on the Disintegration of Liquid Jets," *Ind. Eng. Chem.*, Vol. 47, No. 9, 1955, pp. 1690-1701.

8. Ranz, W.E., "Some Experiments on Orifice Spray," *Canad. J. Chem. Engineering*, Vol. 36, 1958, p. 175.

9. Reitz, R.D., and Bracco, F.V., "Mechanism of Atomization of a Liquid Jet," *Encyclopedia of Fluid Mechanics*, (N.P. Cheremisinoff, Ed.), Vol. 3, Gulf Pub., Houston, TX, 1986, pp. 233-249.

10. Torda, T.P. and Schmidt, L.A., "One-Dimensional Unsteady Aerothermochemical Analysis of Combustion Instability of Liquid Rocket Engines," *Pyrodynamics*, Vol. 1, Gordon and Breach, Science Publishers, Ltd., 1964, pp. 89-111.

11. Culick, F.E, "Combustion Instabilities in Liquid Propulsion Systems - An Overview", Caltech (1988)

12. Crocco, L., "Theoretical Studies on Liquid-Propellant Rocket Instability", Tenth International Combustion Symposium, pp. 1101-1128 (1965).

13. Candel, Poinsot, "A Tutorial on Acoustics", Ecole Central, Paris (1987).

B.8 PAPERS AND PRESENTATIONS FROM THIS AFOSR SUPPORT

1. A. Ghafourian, R. McGuffin, S. Mahalingam, and J.W. Daily,"Dynamic Response to Acoustic Perturbation of an Atomizing Coaxial Jet in a Liquid Rocket Engine", 31st Aerospace Sciences Meeting, Reno, NV, AIAA 93-0232, January 11-14, 1993.

2. J.W Daily and S. Mahalingam, "Dynamic Atomization in Liquid Rocket Engines", Contractors Meeting in Propulsion, Sponsored by Air Force Office of Scientific Research, La Jolla, CA, June 15-19, 1992.

3. A. Ghafourian, C. Huynh, S. Mahalingam, J.W Daily, "Preliminary Results on the Effect of Acoustic Perturbation on an Atomizing Coaxial Jet", ILASS-AMERICAS '92, 5th Annual Conference on Liquid Atomization and Spray Systems, San Ramon, CA, May 18-20, 1992.

4. C. Huynh, A. Ghafourian, S. Mahalingam, and J.W. Daily,"Dynamic Behavior of Atomizing Jets in

Liquid Rocket Engines," *Western State Section of the Combustion Institute*, Spring, 1992.

5. C. Huynh, A. Ghafourian, S. Mahalingam, and J.W. Daily, "Combustor Design for Atomization Study in Liquid Rocket Engines," *30th Aerospace Sciences Meeting,* Reno, NV, AIAA 92-0465, January 6-9, 1992.

6. S. Hevert and S. Mahalingam, "Understanding Linear Theory Results for Liquid Jet Instability," *Western States Section of the Combustion Institute*, Fall, 1991.

7. C. Huynh, A. Ghafourian, S. Mahalingam, and J.W. Daily, "Design and Testing of a Uni-Element Liquid Rocket Engine," *Western States Section of the Combustion Institute*, Fall, 1991.

8. S. Hevert, S. Mahalingam, and J.W. Daily, "Velocity Profile Effects on the Stability of a Liquid Jet," WSS/CI 91-41, *Western States Section of the Combustion Institute*, Spring, 1991.

9. A. Ghafourian, C. Huynh, S. Mahalingam, and J.W. Daily, "Combustor Design for Study of Combustion Instability in Liquid Rocket Engines," WSS/CI 91-54, *Western States Section of the Combustion Institute,* Spring, 1991.

10. A. Ghafourian, S. Mahalingam, H. Dindi, and J.W. Daily, "A Review of Atomization in Liquid Rocket Engines," AIAA 91-0283, *29th Aerospace Sciences Meeting*, Reno, NV, January 7-10, 1991.

11. A. Ghafourian, J.W. Daily, S. Mahalingam, and H. Dindi, "Atomization in Liquid Rocket Engines," *27th JANNAF Combustion Subcommittee Meeting,* Cheyenne, WY, November 5-9, 1990.

12. A. Ghafourian, S. Mahalingam, H. Dindi, and J.W. Daily, "Atomization in Liquid Rocket Engines," *23rd Symposium (International) on Combustion,* Orleans, France, July 22-27, 1990.

B.9 SEMINARS AND PRESENTATIONS NOT INCLUDED ABOVE

1. J.W. Daily, "Dynamic Response to Acoustic Perturbation of an Atomizing Coaxial Jet in a Liquid Rocket Engine," SEP, Vernon, France, March 25, 1992.

2. S. Mahalingam, "Propulsion Research," NASA/Lewis Research Center, Cleveland, OH, July 1991.

3. S. Mahalingam, "Research on Turbulent Combustion and Propulsion," National Renewable Energy Laboratory (NREL), Golden, CO, October 1991.

B.10 PERSONNEL

1. Akbar Ghafourian, Ph.D. candidate, University of Colorado, Boulder.

2. Can Huynh, visiting scholar, Ecole Centrale Paris, France.

3. Rom McGuffin, graduate student, University of Colorado, Boulder.

4. Franz-Josef Kahlen, visiting scholar, Technical University of Aachen, Germany.

Table 1: ρ_l/μ_l of Liquids

	LOX (crit)	LOX (sat)	H_2O_2	Water	Ethanol	Freon 113	Jet A	Shell wax
$\frac{\rho_l}{\mu_l} \times 10^6$	2.6	7.2	1.0	1.1	0.8	2.3	0.5	0.4

Table 2: ρ_g/σ_l of Different Gas Liquid Combinations

	LOX(crit)/GH2	LOX(sat)/GH2	H_2O_2/propane	Ethanol/O_2	Water/R13B
$\frac{\rho_g}{\sigma_l}$	1176	375	80	195	216

	Freon113/R13b	H_2O_2/ propane, R13B	ethanol/O_2, Air	Water, ethanol/R13B
$\frac{\rho_g}{\sigma_l}$	947	151	180	782

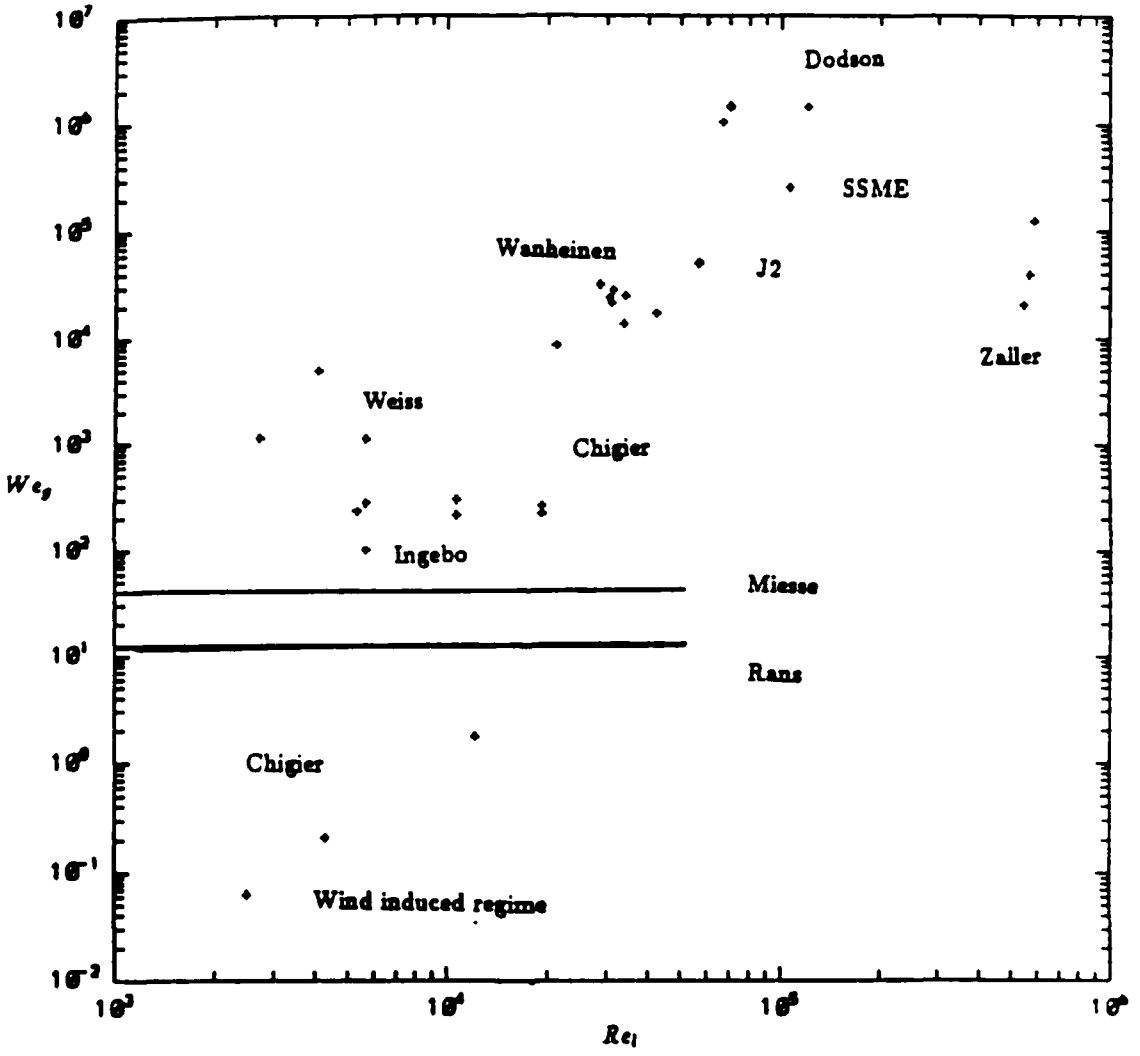

Figure 1: Re_l-We_g Diagram of Some Previous Experimental Studies on Coaxial Injectors

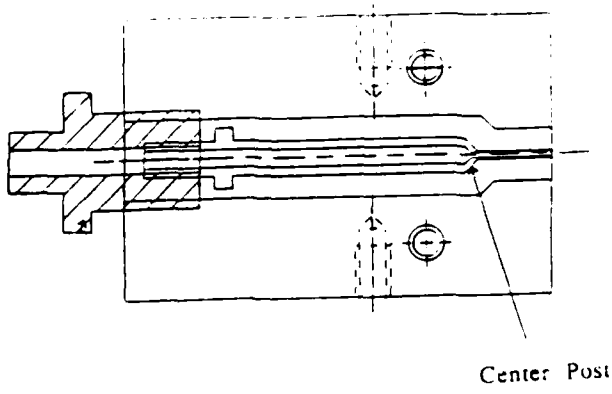

Figure 2: Injector head, coaxial injector

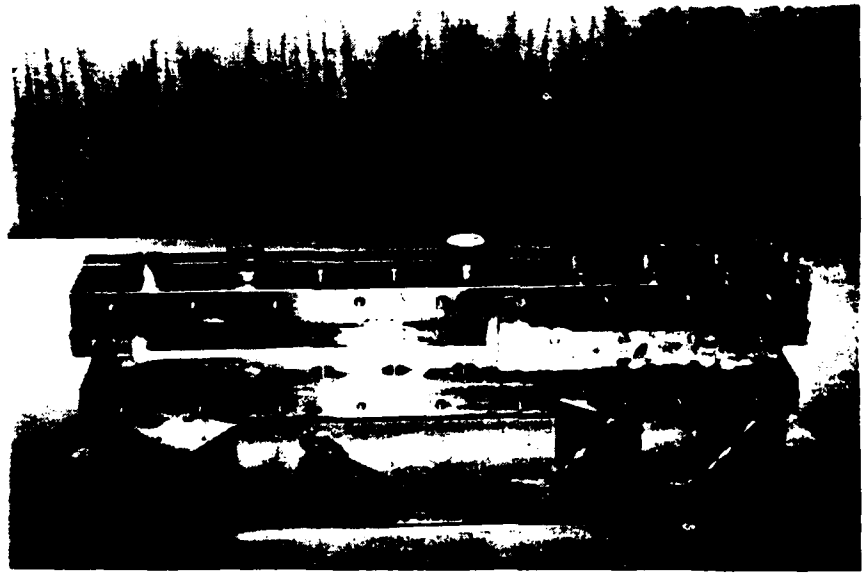

Figure 3. Picture of Combustion Chamber

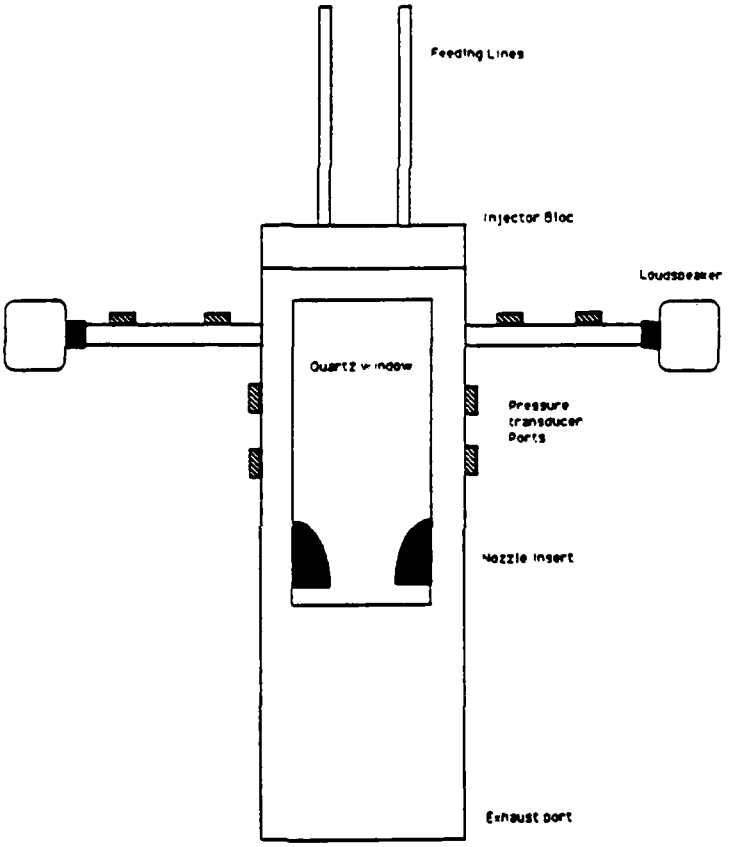

Figure 4: Combustor Sketch for Transverse Mode Forcing

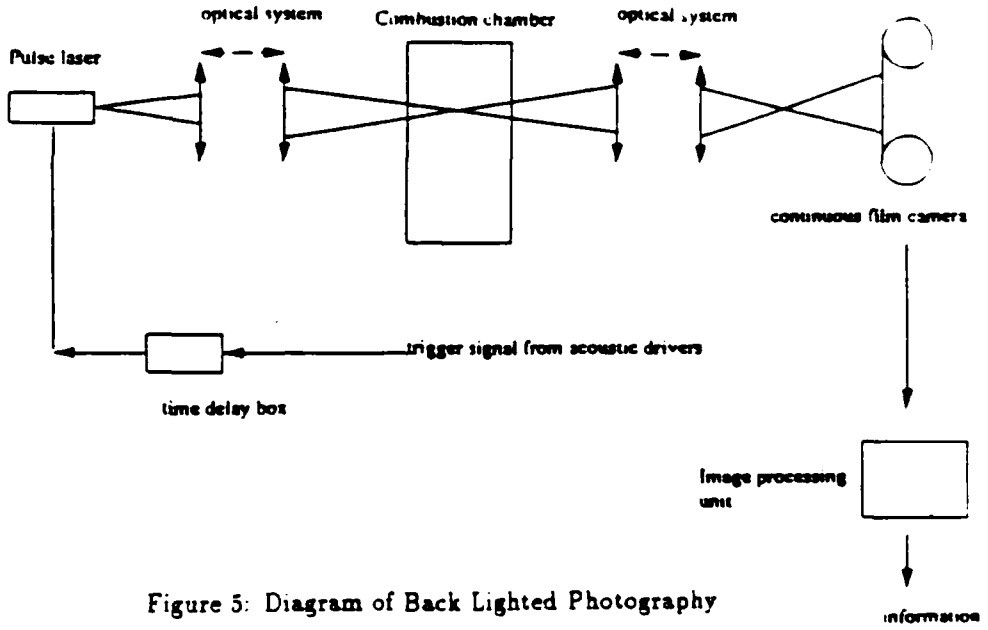

Figure 5: Diagram of Back Lighted Photography

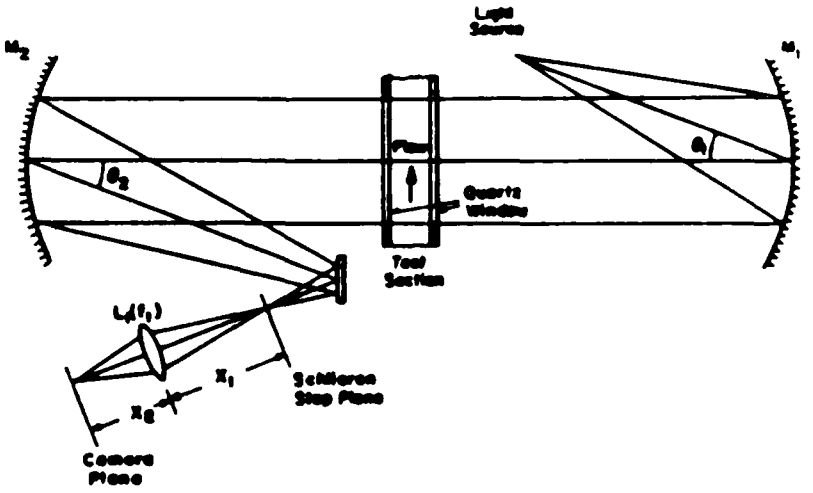

Figure 6: Diagram of Schlieren Imaging System

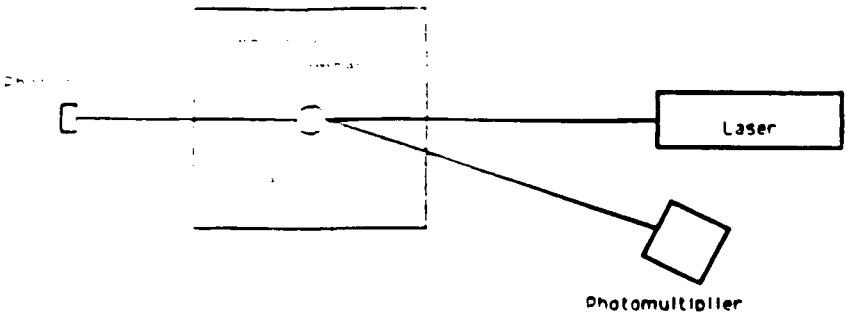

Figure 7: Schematic of Laser Backscattering and Extinction System

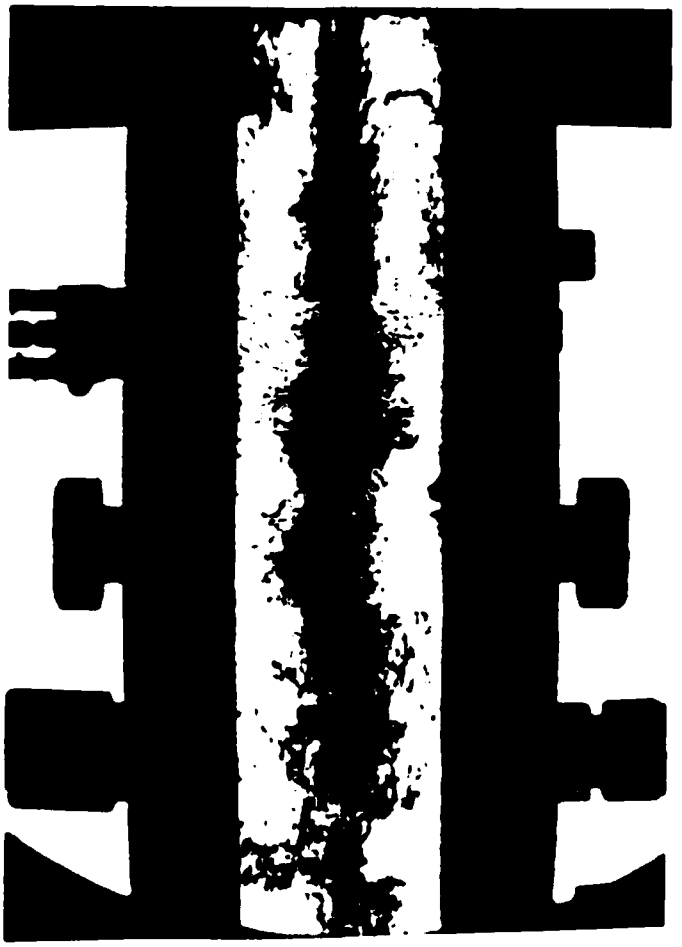

Figure [illegible] Hot Test

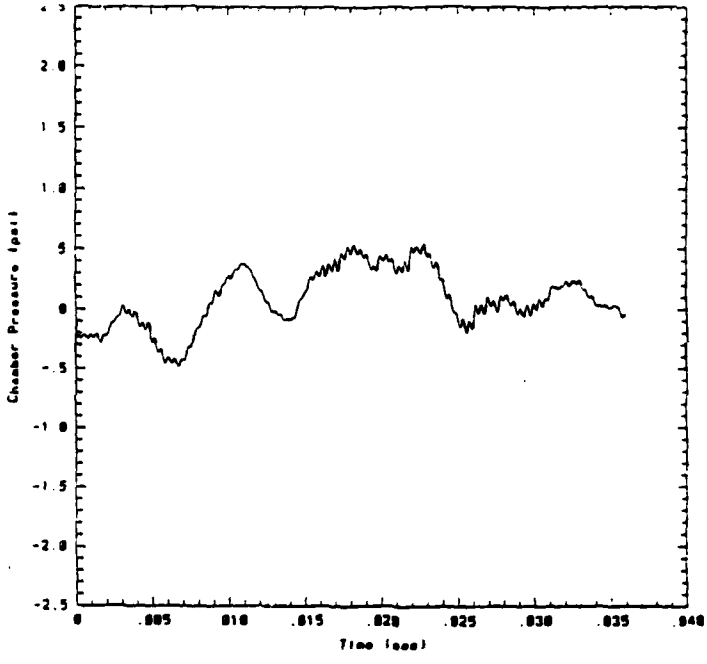

Figure 9: Unexcited chamber pressure, gas phase velocity = 93 m/s, liquid velocity = 15 m/s, equivalence ratio = 7.4

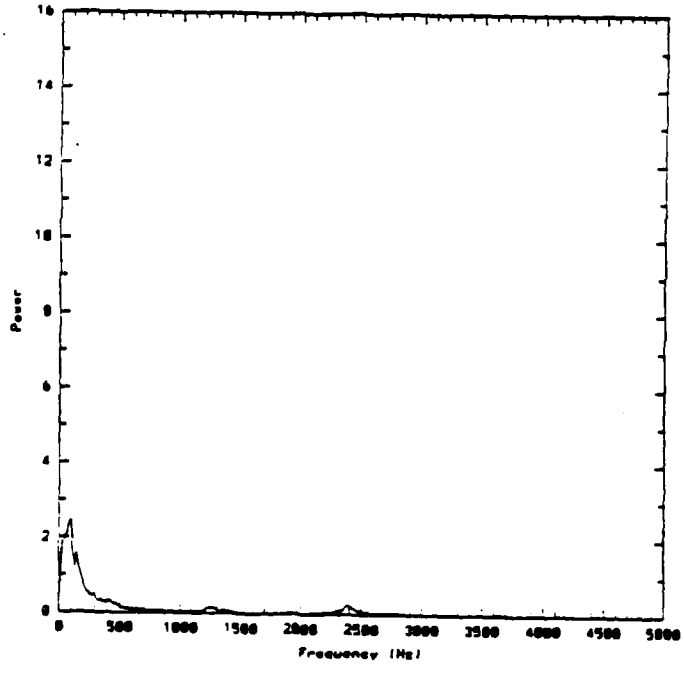

Figure 10: Power Spectrum, unexcited, gas phase velocity = 93 m/s, liquid velocity = 15 m/s, equivalence ratio = 7.4

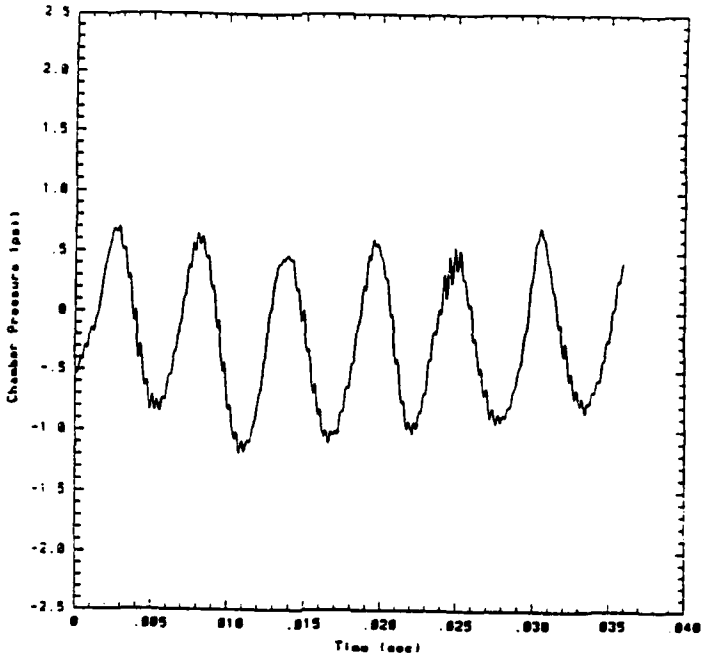

Figure 11: Excited chamber pressure, gas phase velocity = 93 m/s, liquid velocity = 15 m/s, equivalence ratio = 7.4

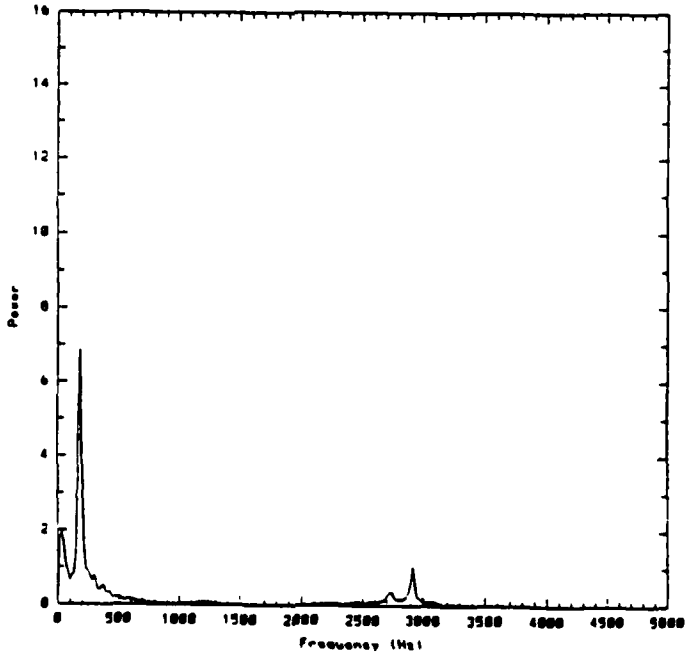

Figure 12: Power Spectrum, excited, gas phase velocity = 93 m/s, liquid velocity = 15 m/s, equivalence ratio = 7.4

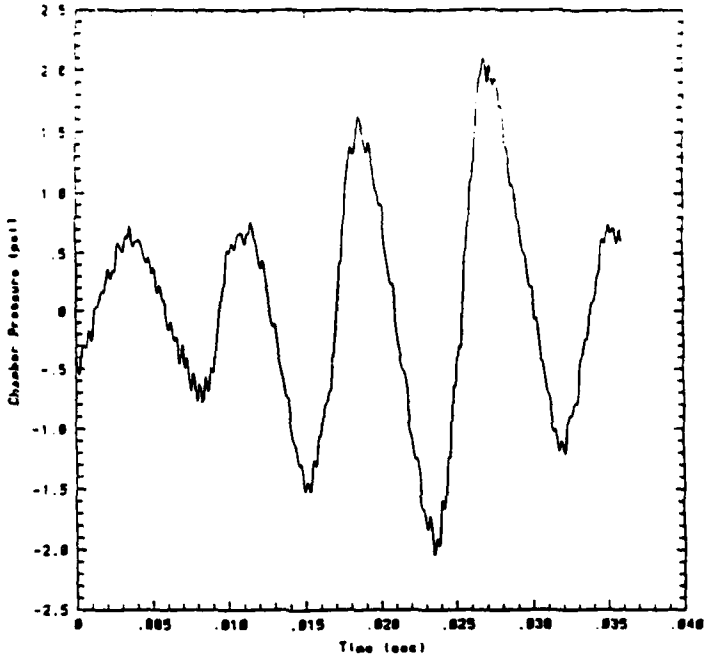

Figure 13: Unexcited chamber pressure, gas phase velocity = 93 m/s, liquid velocity = 15 m/s, equivalence ratio = 3.8

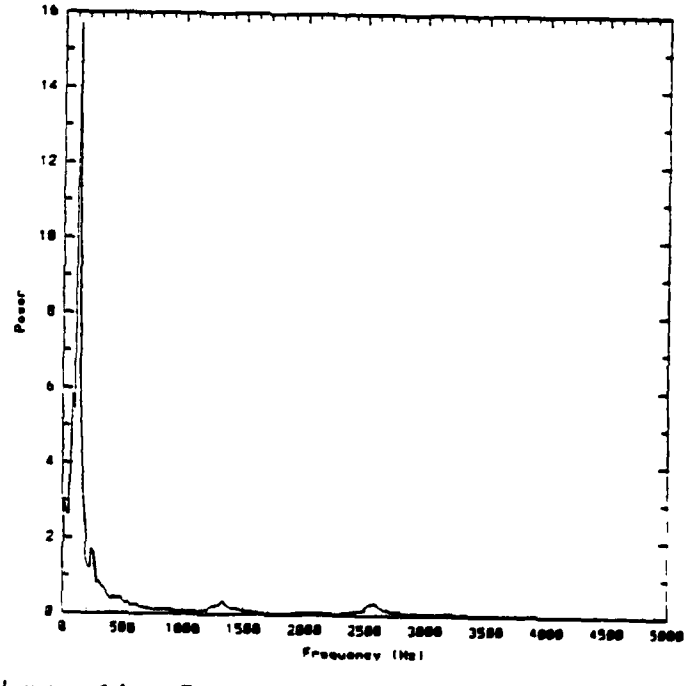

Figure 14: Power Spectrum, unexcited, gas phase velocity = 93 m/s, liquid velocity = 15 m/s, equivalence ratio = 3.8

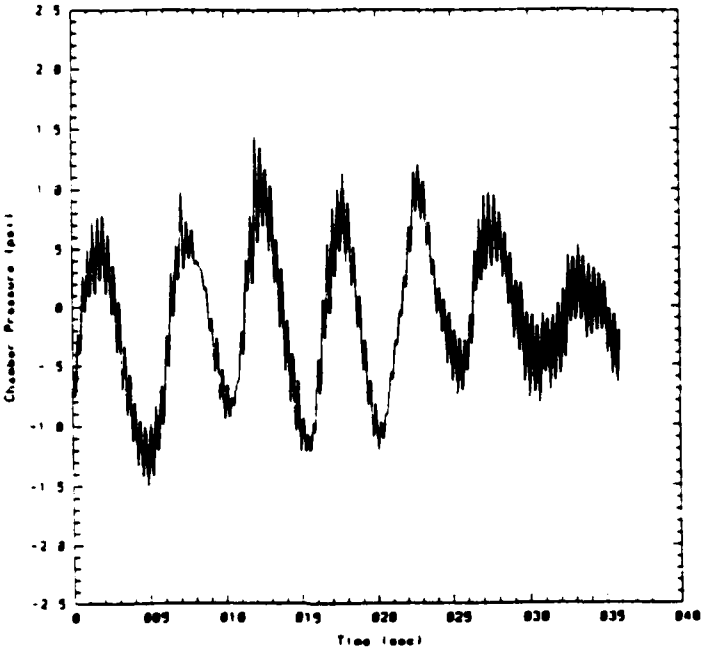

Figure 15: Excited chamber pressure, gas phase velocity = 93 m/s, liquid velocity = 15 m/s, equivalence ratio = 3.8

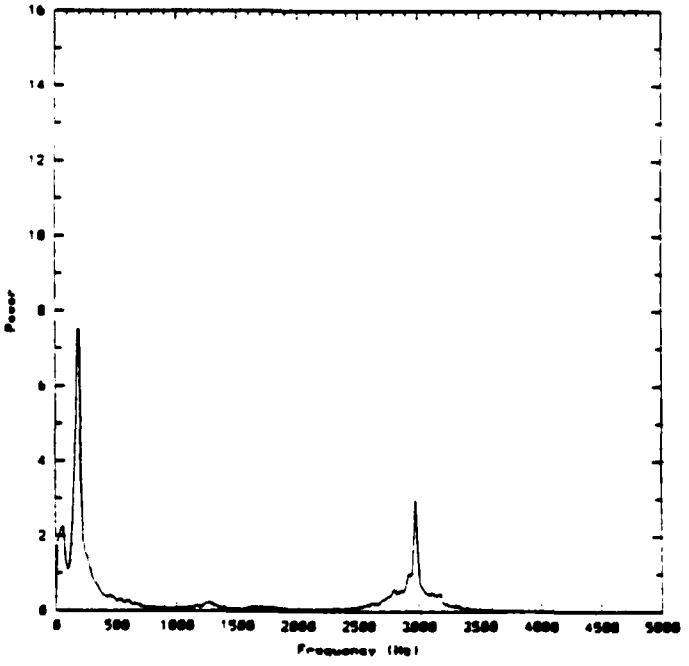

Figure 16: Power Spectrum, excited, gas phase velocity = 93 m/s, liquid velocity = 15 m/s, equivalence ratio = 3.8

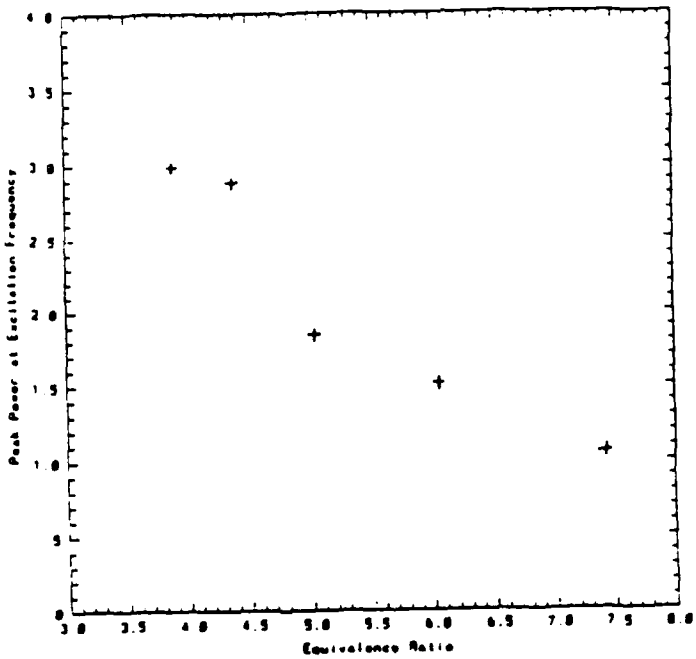

Figure 17: Peak Power Spectrum Amplitude at Excitation Frequency vs. Equivalence Ratio

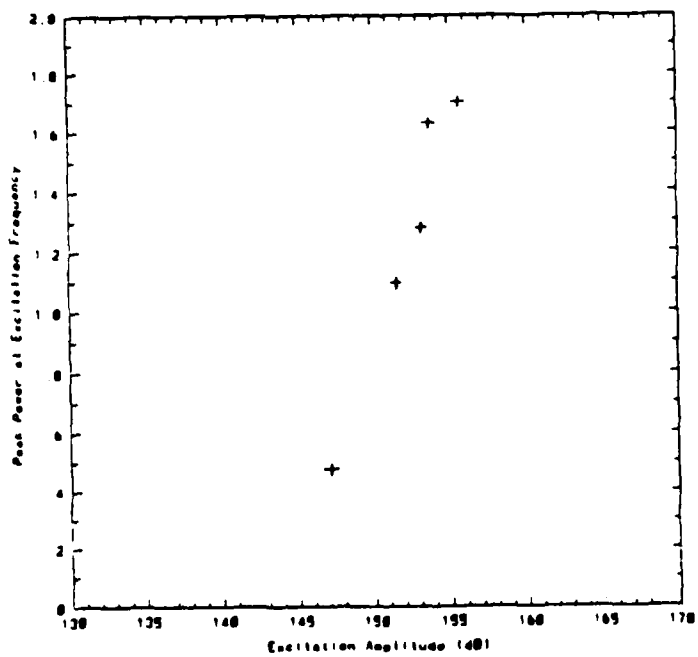

Figure 18: Peak Power Spectrum Amplitude at Excitation Frequency vs. Excitation Amplitude